

Single-electron capture and direct scattering in $\text{He}^{2+} + \text{D}_2$, O_2 , and N_2

S. J. Martin, J. Stevens,* and E. Pollack

Department of Physics, University of Connecticut, Storrs, Connecticut 06269-3046

(Received 17 September 1990)

Single-electron capture and direct scattering are investigated in He^{2+} collisions with D_2 , O_2 , and N_2 molecules. For D_2 , measurements are made at 2.0, 3.0, and 4.0 keV. At the smallest scattering angles, only the exothermic $\text{He}^+(1s) + \text{D}_2^{+*}$ channel is excited. Capture to $\text{He}^+(n=2) + \text{D}_2^+(X)$ is found to have a threshold at a reduced scattering angle τ near 2 keV deg and its contribution rises rapidly. The direct scattering is primarily elastic. O_2 is studied at 4.0 keV and the capture at small angles is dominated by the quasis resonant $\text{He}^+(n=2) + \text{O}_2^+(X^2\Pi_g)$ and the exothermic $\text{He}^+(1s) + \text{O}_2^{+*}$ channels. The direct-scattering channel is electronically elastic for $\tau < 1.6$ keV deg. N_2 is studied at 4.0 keV. For $\tau > 1.0$ keV deg electron capture dominates the collision. The capture is predominantly exothermic for $\tau < 1.2$ keV deg.

I. INTRODUCTION

At the present time, we have a reasonable understanding of the underlying dynamics in ion-atom and atom-atom collisions. Our understanding of collisions involving molecular targets is not as fully developed and is best guided by studying simple systems. The several charge states of the helium- H_2 collision system are ideal "simple systems" since they present challenges to the theory but are still tractable. There has been considerable work done on them: the direct scattering and electron capture in $\text{He}^+ + \text{H}_2$ has been extensively studied,¹⁻³ and there have been studies on $\text{He} + \text{H}_2$ (Refs. 3 and 4) and $\text{H}_2^+ + \text{He}$.^{5,6} This earlier work has led to some understanding of the interactions in the neutral and singly charged He- H_2 cases. The major aspect of our present study involves the doubly charged $\text{He}^{2+} + \text{D}_2$ case. D_2 is used since the electronic processes are identical to those in H_2 targets but the heavier isotope provides kinematic advantages including projectile scattering over a larger range of laboratory angles. For a fixed-apparatus angular resolution this results in improved cross-section measurements.

In this study, we investigate the single-electron capture as well as the direct-scattering channels. The single-electron capture in $\text{He}^{2+} + \text{D}_2$ collisions involves both endothermic and exothermic processes. The earlier work on electron capture in singly charged $\text{He}^+ + \text{H}_2$ collisions resulted in some interesting conclusions for the exothermic capture channels. These channels were found to be very weakly excited (compared to electron capture to endothermic final channels), to exhibit a strong energy dependence, and were attributed to a Demkov-type coupling.⁷ One goal of the present study is to determine whether the exothermic capture processes are also weak in $\text{He}^{2+} + \text{D}_2$.

In addition to improving our understanding by studying "simple systems," it is often useful to establish common characteristics of excitation processes. In this context it is particularly interesting that He^+ collisions with

N_2 and O_2 showed⁸ that the exothermic capture channels exhibit the same weak excitation and strong energy dependence as was found for H_2 targets. An important conclusion of these earlier studies is that the exothermic channels are only weakly excited in all the systems. In the present work, a limited study of the single-electron capture from N_2 and O_2 is also undertaken in order to test the relative importance of the exothermic capture channels for the He^{2+} collisions. Direct-scattering results are also presented.

To date, most of the work done on He^{2+} collisions with D_2 , O_2 , and N_2 has been experimental and there are only few theoretical predictions available for them. In this paper we report differential cross sections for both the single-electron capture and the direct-scattering channels at energies of 2, 3, and 4 keV for D_2 and at 4 keV for O_2 and N_2 .

II. EXPERIMENTAL ARRANGEMENT AND TECHNIQUES

The basic experimental arrangement has been previously described⁹ and is only outlined here. Ions are extracted from a source operating with ultra-high-purity He. They are mass analyzed using a magnetic mass spectrometer and then collimated into a monoenergetic beam. The beam enters a cell containing the target gas and scatters through an angle θ under single-collision conditions. The scattered ions then enter the detector chamber, where they are charge-state and energy analyzed by a parallel-plate electrostatic energy analyzer.

Since the single-electron capture involves a change of charge state, the incident beam cannot provide the energy reference which is needed to determine ΔE , the energy loss. In this work we obtain the necessary reference from the 11-eV peak, reported by Chen *et al.*,¹⁰ in $\text{He}^{2+} + \text{He} \rightarrow \text{He}^+(1s) + \text{He}^+(n=2)$ collisions. The use of this energy reference gives results that are consistent with the known properties of our analyzer.

Electron capture in keV energy ion-molecule collisions

generally involves a "Franck-Condon" transition from the initial molecular state. Since the potential energy of the final molecular ion state may vary significantly over the range of internuclear separations for the initial ground vibrational state, the measured energy-loss spectra are expected to be broad. This can result in an overlap of the spectra from excitation of different electronic levels of the He^+ .

In the present study we investigate the direct scattering, the single-electron capture to $\text{He}^+(1s)+\text{D}_2^{+*}$, $\text{He}^+(n=2)+\text{D}_2^+(X)$, and the summed (over all contributing states) single-capture processes in O_2 and N_2 . For each collision system, the summed direct and summed single-capture cross sections are determined after necessary corrections for geometry, beam intensity, scattering gas pressure, etc. are made. From these summed results, cross sections for the individual processes (when reported) are determined using the energy spectra. At a given angle θ , the number of counts in the peak corresponding to a final channel, such as $\text{He}^+(1s)+\text{D}_2^{+*}$, is divided by the total number of counts in the single-electron-capture spectrum. The cross section for the channel is the product of the summed cross section and the count ratio. The relative count rates for the summed direct- and single-capture processes are measured at a fixed angle thus allowing a direct comparison of these cross sections. Final results are presented in terms of $\rho [= \theta^2 \sigma(\theta)$ at small angle], the reduced cross section, versus $\tau (=E\theta)$, the reduced scattering angle,¹¹ for the channels studied.

III. EXPERIMENTAL RESULTS

A. $\text{He}^{2+} + \text{D}_2$

Single-electron capture is studied at energies of 2.0, 3.0, and 4.0 keV. Figure 1(a) shows an energy spectrum from $E=4.0$ -keV, $\theta=0.5^\circ$ $\text{He}^{2+} + \text{D}_2 \rightarrow \text{He}^+$ collisions. This small-angle spectrum shows a dominant exothermic peak (A') with a maximum at an excitation energy $Q=-9$ eV. A' is attributed to electron capture to $\text{He}^+(1s)$ and excited D_2^{+*} . Although the width of the peak is large compared to that of the incident beam, the state identification can be made. Figure 1(b) at a scattering angle of 1.0° shows the presence of a second peak (B') which is found in the spectra for $\tau > 2.0$ keV deg. This peak corresponds to electron capture to the endothermic $\text{He}^+(n=2)+\text{D}_2^+(X^2\Sigma_g^+)$, $Q=3.5$ -eV, channel. Peak B' is the lowest state in the Rydberg series resulting in capture to $\text{He}^+(n \geq 2)$ with a recoil target in the bound $\text{D}_2^+(X)$ state. The contribution from these endothermic electron-capture processes is found to increase with scattering angle. Capture to $\text{He}^+(n=2)+\text{D}_2^+(X)$ is, however, found to be the dominant endothermic process in the angular range investigated. For $\tau > 3.2$ keV deg there are weaker (and unresolvable) contributions from states in the Rydberg series $\text{He}^+(n > 2)+\text{D}_2^+(X)$ and from processes with $Q > 16$ eV which result in $\text{He}^{+*} + \text{D}_2^{+*}$. Capture to $\text{He}^+(1s)+\text{D}_2^+(X)$ is not found. At the other energies investigated, the exothermic peak (A') is again seen to be dominant at small angles. The excitation of $\text{He}^+(n=2)+\text{D}_2^+(X)$ is found to have

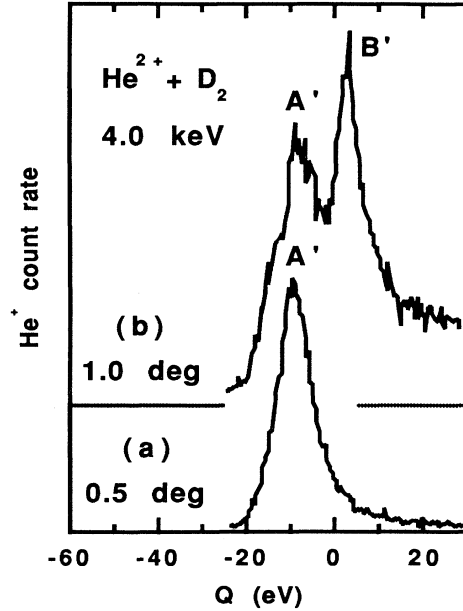


FIG. 1. Energy spectra for electron capture in 4.0-keV $\text{He}^{2+} + \text{D}_2$ collisions. Peak A' , with a maximum at $Q=-9$ eV, is predominantly due to capture to $\text{He}^+(1s)+\text{D}_2^{+*}$ (these processes are exclusively exothermic). Peak B' is attributed to capture to $\text{He}^+(n=2)+\text{D}_2^+(X)$, which is endothermic with a $Q=3.5$ eV. (a) $\theta=0.5^\circ$ dominated by A' . (b) $\theta=1.0^\circ$; the B' and A' channels are comparable. The absolute count rate for the data in (b) is a factor of 10 less than for (a).

a threshold near $\tau=2.0$ keV deg at the 2.0-, 3.0-, and 4.0-keV energies studied.

The direct scattering is studied at the three energies. A typical spectrum for the direct scattering is shown in Fig. 2, where peak A corresponds to electronically elastic collisions. Electronically inelastic processes are found to be weak at all three energies in the angular range studied.

The reduced differential cross sections for electron capture to $\text{He}^+(1s)+\text{D}_2^{+*}$, $\text{He}^+(n=2)+\text{D}_2^+(X)$ and for elastic scattering are shown in Fig. 3 at an energy $E=4.0$ keV. The elastic scattering and the exothermic $\text{He}^+(1s)+\text{D}_2^{+*}$ channels have a similar angular dependence in their cross sections and are the dominant processes at small angles. Electron capture to $\text{He}^+(n=2)+\text{D}_2^+(X)$ shows a threshold near 2.0 keV deg, is weak at small angles, and becomes comparable to the other processes near 5 keV deg.

B. $\text{He}^{2+} + \text{O}_2$

Single-electron capture is studied at 4.0 keV. Figure 4 shows a spectrum at $\theta=0.1^\circ$. At small angles, the electron capture is dominated by the exothermic $\text{He}^+(n=2)+\text{O}_2^+(X^2\Pi_g)$ channel (A') with $Q=-1.3$ eV. A second peak, B' , corresponding to Q values from -5 to -20 eV, is also seen, and results from capture to $\text{He}^+(1s)$ and excited (including autoionizing) states of O_2^+ .¹² Peak B' increases in importance with increasing

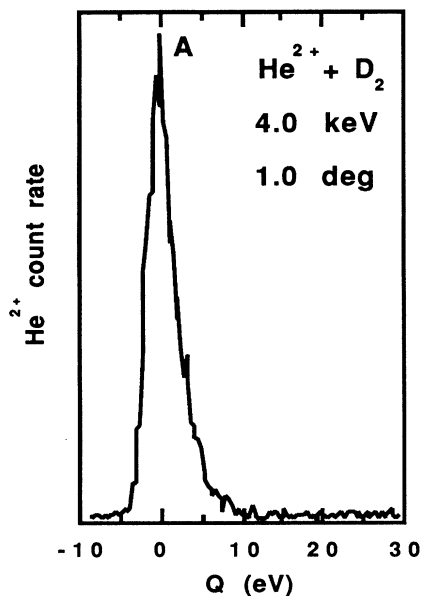


FIG. 2. Energy spectrum for 4.0-keV, $\theta=1.0^\circ$, direct scattering in $\text{He}^{2+} + \text{D}_2$ collisions. The scattering is dominated by *A*, the elastic channel. Inelastic scattering is very weak at all angles in the range studied.

scattering angle. No capture to $\text{He}^+(1s) + \text{O}_2^+(X)$ is seen. For $\tau > 2.0$ keV deg the electron capture is dominated by endothermic processes which cannot be resolved.

An energy spectrum for the direct scattering in 4.0-keV $\text{He}^{2+} + \text{O}_2$ is shown in Fig. 5. The elastic peak is labeled *A*. Electronically inelastic processes are found to be weak for $\tau < 1.6$ keV deg. At $\tau = 2.4$ keV deg, inelastic processes account for approximately 10% of the direct scattering. In our τ range the inelastic processes result predominantly in excitation of the O_2 target with $5 \text{ eV} < Q < 10 \text{ eV}$, corresponding to both bound and dissociating states of the O_2 .

Since the individual states are not resolvable, only reduced differential cross sections for the summed single-

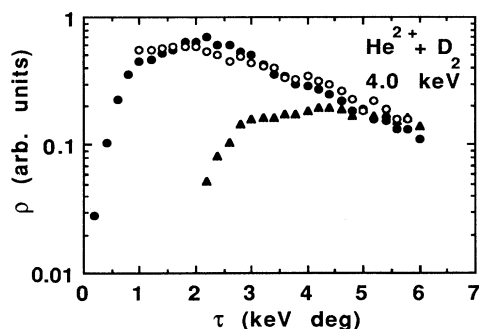


FIG. 3. The reduced cross sections for $\text{He}^{2+} + \text{D}_2$ scattering at 4.0 keV; (○) elastic scattering, (●) single-electron capture to $\text{He}^+(1s) + \text{D}_2^+*$, and (▲) single-electron capture to $\text{He}^+(n=2) + \text{D}_2^+(X)$.

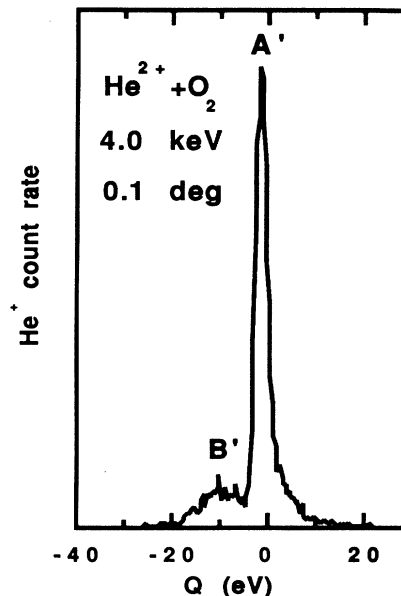


FIG. 4. Energy spectrum for single-electron capture in 4.0-keV, $\theta=0.1^\circ$, $\text{He}^{2+} + \text{O}_2$ collisions. Peak *A'* is due to capture to $\text{He}^+(n=2) + \text{O}_2^+(X)$, which is quasiresonant ($Q = -1.3 \text{ eV}$). Peak *B'* is due to capture to exothermic $\text{He}^+(1s) + \text{O}_2^+*$. Peak *B'* includes processes with Q values from -5 to -20 eV in the angular range studied and results mostly from excitation of O_2^+ autoionizing states.

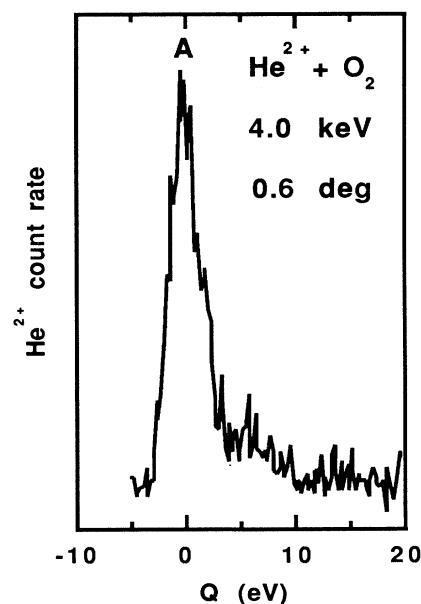


FIG. 5. Energy spectrum for direct scattering in 4.0-keV, $\theta=0.6^\circ$, $\text{He}^{2+} + \text{O}_2$ collisions. Peak *A* is due to elastic scattering. Inelastic processes with $5 \text{ eV} < Q < 10 \text{ eV}$ are found. These result from excitation of O_2 to both bound and dissociating states.

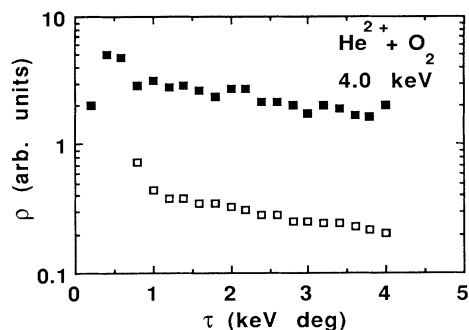


FIG. 6. Reduced cross sections for 4.0-keV $\text{He}^{2+} + \text{O}_2$ collisions: (\square), summed direct scattering; (\blacksquare), summed single-electron capture. The arbitrary units are the same as reported in Fig. 3, allowing a direct comparison with D_2 .

electron-capture channels and for the summed direct scattering channels are shown in Fig. 6.

C. $\text{He}^{2+} + \text{N}_2$

The single-electron capture in small-angle 4.0-keV $\text{He}^{2+} + \text{N}_2$ collisions is dominated by a single wide peak which has a maximum at $Q = -9$ eV and results from capture to $\text{He}^+(1s)$ and excited (including autoionizing) states of N_2^+ .¹² Figure 7 shows a typical spectrum at $\theta = 0.1^\circ$. Endothermic electron capture resulting in excited states of both the projectile and target becomes important for $\tau > 1.2$ keV deg and rapidly dominates the collision. Electron capture to the $\text{He}^+(1s) + \text{N}_2^+(X)$ ground

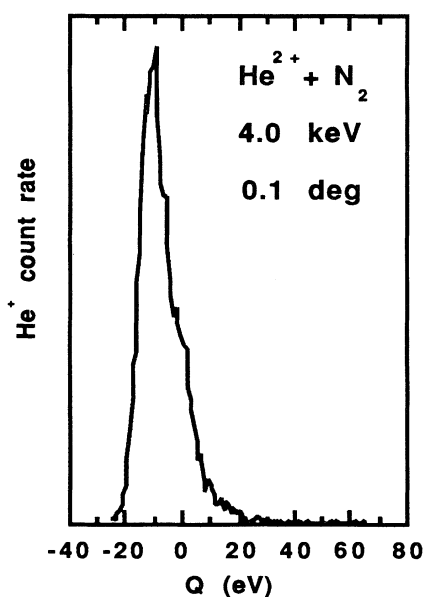


FIG. 7. Energy spectrum for single electron capture in 4.0-keV, $\theta = 0.1^\circ$, $\text{He}^{2+} + \text{N}_2$ collisions. The scattering is dominated by a single peak with a maximum at $Q = -9$ eV. This peak primarily results from exothermic processes following capture to $\text{He}^+(1s)$ and excited (including autoionizing) states of N_2^+ .

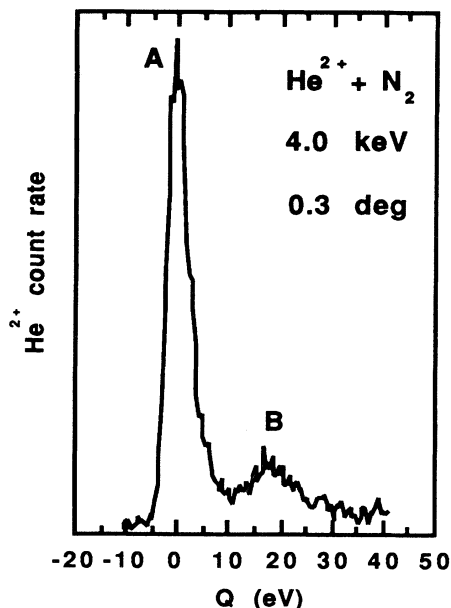


FIG. 8. Energy spectrum for direct scattering in 4.0-keV, $\theta = 0.3^\circ$, $\text{He}^{2+} + \text{N}_2$ collisions. Peak *A* is due to elastic scattering. The inelastic peak *B* has a maximum at $Q = 19$ and includes processes with Q values from 13 to 26 eV. Processes with $Q < 16$ eV result in excited states of N_2 (both bound and dissociating). Processes with $Q > 16$ eV result in autoionizing states of N_2 .

state is not found.

The direct scattering is studied at 4.0 keV. Inelastic processes are seen to occur for $\theta > 0.1^\circ$. An energy spectrum for the direct scattering at $\theta = 0.3^\circ$ is shown in Fig. 8 where an inelastic peak, *B*, is seen. Peak *B* has a maximum at 19 eV and includes processes with Q values ranging from 13 to 26 eV. The processes with $Q < 16$ eV are consistent with the excitation of N_2 to both bound and dissociating states. For $Q > 16$ eV, excitation of autoionizing states may contribute. Direct inelastic pro-

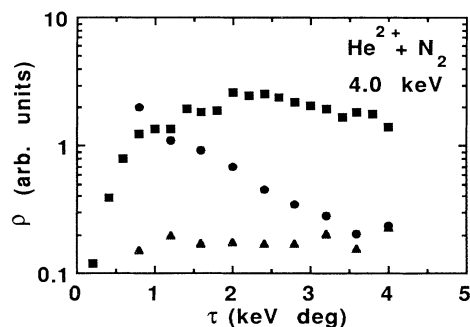


FIG. 9. Reduced cross sections for 4.0-keV $\text{He}^{2+} + \text{N}_2$ collisions, (\bullet), elastic scattering; (\blacktriangle), summed direct inelastic-scattering channels, (\blacksquare), summed single-electron capture. The arbitrary units are the same as reported in Fig. 3, allowing a direct comparison with D_2 .

cesses become stronger with increasing scattering angle. At $\theta=0.2^\circ$, inelastic collisions account for about 7% of the direct scattering. The ratio increases monotonically out to 1.0° , where they are 50% of the direct scattering.

The reduced differential cross sections for elastic scattering, the summed direct inelastic scattering, and the summed single-electron-capture processes are shown in Fig. 9. The single-electron capture is seen to rise sharply at small angles and then level off. At the smallest angles, the elastic scattering is dominant, but its contribution drops off monotonically over the angular range studied. Beyond $\tau=1.2$ keV deg the single-electron capture dominates the collision.

IV. DISCUSSION AND CONCLUSION

There have been a number of studies of single-electron capture in $\text{He}^{2+} + \text{H}_2$ (see as examples Refs. 13–18). The forward scattering was investigated by Kobayashi *et al.*,¹³ who reported a single broad peak with a $Q = -11$ eV. This is in basic agreement with our present results (on D_2), which show a single broad peak (A'), with approximately the same Q , in the forward scattering.

Afrosimov *et al.*¹⁴ studied $\text{He}^{2+} + \text{H}_2$ collisions at energies from 1 to 100 keV and reported total cross sections as a function of energy for five types of processes. For energies $E > 15$ keV, the largest cross section was due to nondissociative capture resulting primarily in $\text{He}^+(n=2) + \text{H}_2^+(X)$. At energies $E < 10$ keV, dissociative capture resulting in $\text{He}^+(1s) + \text{H}_2^{+*}$ was found to be dominant; the cross sections for dissociative and nondissociative charge exchange cross at approximately 12 keV. Total cross sections for these processes were recently measured by Shah *et al.*,¹⁵ who reported some discrepancies with Ref. 14. Afrosimov *et al.* also measured the differential cross sections for the summed endothermic capture channels at energies of 2.15 and 5.4 keV. We find these endothermic processes to be weak compared to both the $\text{He}^+(1s) + \text{D}_2^{+*}$ channel and to elastic scattering at the small angles in our range. Since the total cross sections depend strongly on contributions from small scattering angles, the present results are consistent with dissociative capture processes, having the largest cross sections at low energy.

Theoretical predictions of cross sections in our energy range require a knowledge of the electronic states of the quasimolecule, since transitions are most likely to occur where the energy surfaces have a crossing or avoided crossing. In the case of exothermic capture, the crossing locations can be estimated if they occur at large interparticle separations. This only requires assuming a simple long-range polarization interaction, since the final states are Coulomb repulsive. Crossing points for these processes can then be calculated from the energy defect and the polarizability of the targets that have values of 5.45, 10.6, and $11.8a_0^3$ for D_2 , O_2 , and N_2 , respectively.¹⁹ Capture processes resulting in $\text{He}^+(1s) + \text{D}_2^{+*}$ are exothermic with a range of Q values lower than -3 eV. Electron capture with a $Q = -3$ eV would have a crossing at $9a_0$. A channel with $Q = -6$ eV would have a crossing at $5a_0$; crossing points for more exothermic processes cannot be

calculated without knowing the energy surfaces of $(\text{HeD}_2)^{2+}$, since they occur at small distances. The crossings at large interparticle separation result in the dominance of the exothermic channels at small angles. Capture to $\text{He}^+(n=2) + \text{D}_2^+(X)$ is endothermic by only 3.5 eV, but since the channel is not excited at the large interparticle distances, it has a threshold at a relatively large τ near 2 keV deg.

Although the molecular orbital (MO) model³ has been shown to be inadequate⁵ in describing some aspects of the $(\text{HeH}_2)^+$ collision system, it is of limited use in $\text{He}^{2+} + \text{D}_2$. In this doubly charged case, the lowest-lying $1s_{\text{He}}$ MO has two vacancies (unlike the case shown in Fig. 4 of Ref. 5). The next-higher-lying $1s\sigma_{\text{H}_2}$ MO contains the two electrons initially on the target molecule. At the smallest scattering angles, corresponding to the largest distances, the electron capture involves a two-electron process. During the collision, one electron is excited to an MO such as $2p\sigma_{\text{H}_2}$, and the other makes a transition to the lowest MO, resulting in the excitation of $\text{He}^+(1s) + \text{D}_2^{+*}$. One-electron processes such as those leading to $\text{He}^{+*}(n=2) + \text{D}_2^+(X)$ are found to be weak at the smallest angles. The assumed weakness of one-electron processes is consistent with the strongly elastic direct scattering, since the excitation of direct inelastic channels at the small scattering angles would primarily involve single-electron processes.

Single-electron capture to $\text{He}^+(n=2) + \text{O}_2^+(X^2\Pi_g)$ is exothermic by 1.3 eV, and within our simple model, results from a crossing at $21a_0$. The electron capture at large interparticle separation is consistent with the observed dominance of this channel at small angles. At larger angles, the exothermic single capture results predominantly in $\text{He}^+(1s)$ and autoionizing states of O_2^+ . The endothermic processes have a threshold at $\tau=1$ keV deg and become dominant at larger τ . Since we cannot resolve the large number of states contributing to both the single capture and direct scattering channels, we can only conclude that the summed capture channels dominate at all angles over the direct channels.

$\text{He}^{2+} + \text{N}_2$ was studied by Kobayashi *et al.*,¹³ who reported on the small-angle single-electron capture. The collision was also investigated by Rogers *et al.*,²⁰ who reported on the elastic, simple inelastic, and single-electron capture at energies of 200 and 600 eV. Our direct-scattering results at 4.0 keV show a single inelastic peak, in basic agreement with the earlier results.²⁰ In both studies, the single-electron capture dominates the collision at large τ . Both studies show that the elastic scattering decreases monotonically and the direct inelastic cross section is flat out to 4.0 keV deg, with the two cross sections converging near $\tau=4.0$ keV deg. However, while in the present work the elastic and single-capture cross sections intersect at 1.2 keV deg, extrapolating the results of Rogers *et al.* gives an intersection at $\tau < 1.0$ keV deg. A comparison of the experimental results in these two energy ranges suggests that the excitation is energy dependent.

The O_2 collision is unique among the three cases. The enhancement of the single-electron-capture cross sections

at small angles is due to the low- Q exothermic $\text{He}^+(n=2)+\text{O}_2^+(X^2\Pi_g)$ channel. At $\tau=3.0$ keV deg the electron capture is already dominated by endothermic processes and the summed cross section becomes comparable to that of N_2 . At all angles in O_2 and beyond the smallest angles in N_2 , the direct scattering is substantially weaker than the electron capture.

This study clearly shows that the small-angle exothermic-electron-capture processes involving D_2 , O_2 , and N_2 are not weak. Although the crossings leading to the exothermic electron capture are expected to occur at

large interparticle separation, this alone cannot explain the importance of these channels in small-angle collisions. The capture also depends on the strength of the couplings between the initial and final states. Since the couplings are unknown, the electron-capture results present an interesting problem for theory.

ACKNOWLEDGMENTS

This work was supported under Grant No. PHY-8507736 from the National Science Foundation and by the University of Connecticut Research Foundation.

*Present address: Department of Chemistry and Physical Sciences, Quinnipiac College, Hamden, CT 06517.

¹A. V. Bray, D. S. Newman, and E. Pollack, *Phys. Rev. A* **15**, 2261 (1977).

²W. L. Hodge, Jr., A. L. Goldberger, M. Vedder, and E. Pollack, *Phys. Rev. A* **16**, 2360 (1977).

³D. Doweck, D. Dhuicq, V. Sidis, and M. Barat, *Phys. Rev. A* **26**, 746 (1982).

⁴J. Jakacky, Jr., E. Pollack, R. Snyder, and A. Russek, *Phys. Rev. A* **31**, 2149 (1985).

⁵E. J. Quintana, A. Andriamasy, D. J. Schneider, and E. Pollack, *Phys. Rev. A* **39**, 5045 (1989).

⁶D. H. Jaecks, O. Yenen, M. Natarajan, and D. Mueller, *Phys. Rev. Lett.* **50**, 825 (1983).

⁷Yu. N. Demkov, *Zh. Eksp. Teor. Fiz.* **45**, 195 (1963) [*Sov. Phys. JETP* **18**, 138 (1964)].

⁸D. Doweck, D. Dhuicq, J. Pommier, V. N. Tuan, V. Sidis, and M. Barat, *Phys. Rev. A* **24**, 2445 (1981).

⁹J. Stevens, R. S. Peterson, and E. Pollack, *Phys. Rev. A* **27**, 2396 (1983).

¹⁰Y. H. Chen, R. E. Johnson, R. R. Humphris, M. W. Siegel,

and J. W. Boring, *J. Phys. B* **8**, 1527 (1975).

¹¹Q. C. Kessel, E. Pollack, and W. W. Smith, in *Collisional Spectroscopy*, edited by R. G. Cooks (Plenum, New York, 1978), Chap. 3.

¹²A. C. Hurley, *J. Mol. Spectrosc.* **9**, 18 (1962).

¹³N. Kobayashi, T. Iwai, Y. Kaneko, M. Kimura, A. Matsumoto, S. Ohtani, K. Okuno, S. Takagi, H. Tawara, and S. Tsurubuchi, *J. Phys. Soc. Jpn.* **53**, 3736 (1984).

¹⁴V. V. Afrosimov, G. A. Leiko, and M. N. Panov, *Zh. Tekh. Fiz.* **50**, 519 (1980) [*Sov. Phys. Tech. Phys.* **25**, 313 (1980)].

¹⁵M. B. Shah, P. McCallion, and H. B. Gilbody, *J. Phys. B* **22**, 3983 (1989).

¹⁶R. Hoekstra, A. R. Schlatmann, F. J. de Heer, and R. Morgenstern, *J. Phys. B* **22**, L603 (1989).

¹⁷R. Shingal and C. D. Lin, *Phys. Rev. A* **40**, 1302 (1989).

¹⁸L. Meng, C. U. Reinhold, and R. E. Olson, *Phys. Rev. A* **40**, 3637 (1989).

¹⁹E. W. Rothe and R. B. Bernstein, *J. Chem. Phys.* **31**, 1619 (1959).

²⁰W. T. Rogers, J. W. Boring, and R. E. Johnson, *J. Phys. B* **11**, 2319 (1978).